

The x-ray light valve: A low-cost digital radiographic imaging system

Ivaylo Koprinarov, Christie Ann Webster, Robert D. MacDougall, and J. A. Rowlands^{a)}
*Imaging Research, Sunnybrook Health Sciences Centre, University of Toronto,
2075 Bayview Avenue, Toronto, Ontario M4N 3M5, Canada*

(Received 20 June 2007; accepted for publication 18 September 2007; published 12 November 2007)

In recent years new digital x-ray radiographic and fluoroscopic systems based on large-area flat-panel technology have revolutionized our capability of producing x-ray images. However, such imagers are extraordinarily expensive and their rapid image acquisition capability is not required for many applications such as radiography. Here we report a novel approach to achieve a high-quality digital radiographic system at a cost which is only a small fraction of competitive digital technologies. The results demonstrate that our proposed x-ray light valve system has excellent spatial resolution and adequate sensitivity compared to existing technologies. © 2007 American Association of Physicists in Medicine. [DOI: [10.1118/1.2799490](https://doi.org/10.1118/1.2799490)]

Until recently, medical x-ray imaging systems were typically based on film. In newer systems, large-area flat-panel technology¹ or storage phosphors² enable production of digital radiographic images. Although such digital systems provide many advantages such as excellent image quality, immediate readout, and easily accessible and transferable images, these newer systems have considerably increased initial costs compared to the film technology they are replacing. This makes them unaffordable for all but a few selected procedures and institutions. Different approaches have been considered to make a low-cost x-ray imaging device for digital radiography.³⁻⁵ However, all of these systems are still quite expensive and none have the image quality of flat-panel systems. Here we report a novel approach to achieve a high-quality digital x-ray detector at a cost that is only a small fraction of competitive digital technologies.^{1,2} By combining the well-established and low-cost technologies of amorphous selenium used in xerography with liquid crystals used in displays, we incorporated an x-ray absorption, image formation, and amplification stage within a simple and compact structure.

Our device, the x-ray light valve (XLV), consists of a photoconductor, used as an x-ray to charge transducer, and a liquid-crystal cell, used as an optically-addressed spatial light modulator.^{6,7} This arrangement allows the latent charge image created by the x-rays absorbed in the photoconductor to be made visible and stored in the liquid-crystal cell. The optical image is subsequently digitized by using an external light source and an optical scanner. For practical utility in medical imaging, the photoconductor must have sufficient x-ray absorption, high sensitivity, high image resolution, and low dark current. Therefore, we chose amorphous selenium (a-Se), which is the only practical material currently capable of satisfying these requirements. The clinical suitability of a-Se for medical x-ray imaging has been established previously in connection with xeroradiography.⁸ Currently, it is also used in direct-conversion flat-panel technology.¹ Large area a-Se detectors are feasible and cost-effective because

the photoconductor is amorphous and is made by evaporation techniques. The manufacturing process is well established because of its extensive past use in the photocopy industry.⁹ This is also the case for the liquid-crystal cell, which is based on technology used in liquid-crystal displays.¹⁰ Therefore, our device can be made large enough to meet the size requirements (35×43 cm) for general radiography¹¹ without increased complexity or excessive cost.

The operation of the XLV-based system can be broken down into three steps: exposure, digitization, and reset, as seen in Fig. 1. During the exposure step, a large electric field (10 V/μm) is applied across the XLV. When an x-ray is absorbed in the a-Se, electron-hole pairs are released. The electric field guides the electrons and holes to opposite surfaces of the photoconductor. Since the charges follow the field, the charge image that is collected at the interface of the a-Se and the liquid-crystal cell accurately reproduces the absorbed x-ray intensity pattern. The trapped charges remain at the interface after the exposure is completed and the electric field is removed. The spatial variation of their field induces a static optical image in the liquid-crystal cell, allowing an optical representation of the absorbed x-rays to be obtained. During the digitization step, this optical image is digitized using an external illumination source and an optical scanner readout. In our prototype, we favor a reflective configuration, which has the illumination on the same side of the XLV as the scanner [see Fig. 1(d)] By adjusting the intensity of the readout light, we are able to compensate for any loss of light in the coupling optics. Therefore, the x-ray image can be recorded without a secondary quantum sink.¹² It should be noted that the wavelength of the readout light (~640 nm) is selected so that it will not interact with the photoconductor (i.e., create more electron-hole pairs) and prematurely erase the charge image. A key feature of the XLV is that the charge image remains stored, allowing the optical scanner time to digitize it. Therefore, it is necessary to reset the XLV to eliminate the image charge before a fresh exposure can be

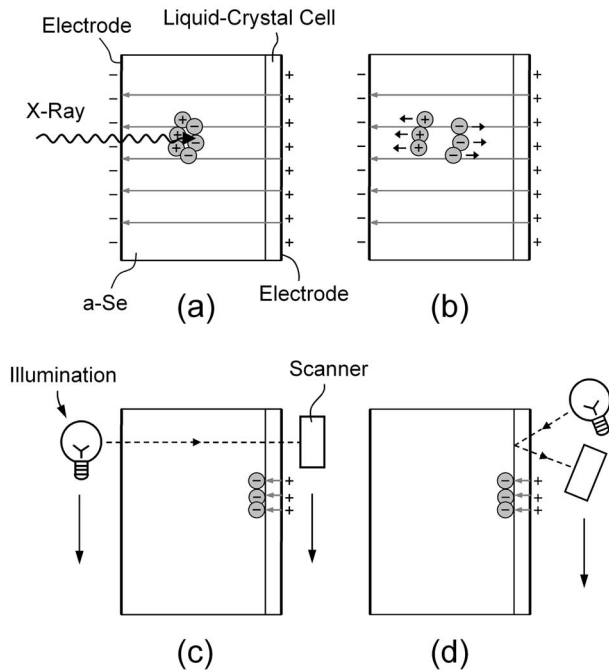


FIG. 1. Basic operation of the XLV. During the exposure, a large potential is applied to the electrodes. (a) X-rays absorbed in the a-Se layer generate electron-hole pairs within a localized region. (b) The large electric field guides the electrons and holes to opposite surfaces of the a-Se. After the exposure is finished and the potential is removed, the charge collected at the a-Se-liquid-crystal interface remains there. The electric field created by the charge image, representing the absorbed x-rays, induces an optically visible image in the liquid-crystal cell. This optical image is digitized using external illumination and an optical scanner in a transmissive (c) or a reflective configuration (d).

made. In this reset step, the photoconductor is uniformly flooded with light, which creates electron-hole pairs in the a-Se (wavelength < 600 nm), also known as actinic light. The charges produced neutralize the image charge and the XLV is ready to acquire a new x-ray image.

The liquid-crystal cell for our device is similar to those in reflective liquid-crystal displays.¹³ It is based on the phase retardation effect, also known as electrically controlled birefringence, with a parallel orientation of the top and bottom alignment layers (homogeneous cell) and an input polarizer oriented 45° to the alignment of the liquid crystal. In our prototypes, the a-Se is evaporated on one of two ITO-covered glass substrates (0.5 mm) used to make the cell. The alignment layer (Rolic Technologies) is then spin coated on both surfaces and formed by using polarized UV light. Adhesive is placed around the perimeter of one of the substrates, allowing an opening for the liquid crystal to be added later. After one of the surfaces is sprayed with spacers, both parts are subsequently put together and placed in a press to maintain the correct cell gap while the adhesive cures. The XLV is then filled with liquid-crystal (ZLI 4792, Merck) by capillary action and the opening is sealed.

Since liquid-crystal cells are not sensitive below a certain threshold voltage, a small potential (~ 1 – 2 V) can be applied during the digitization step to bring the liquid-crystal cell to the threshold of its operating characteristic. Thus the

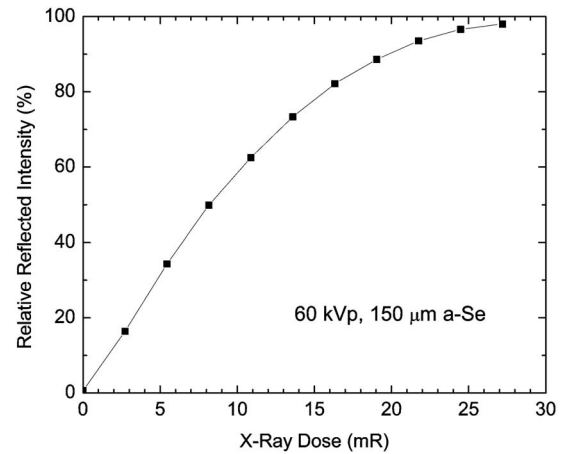


FIG. 2. XLV intensity transfer function measured experimentally. For this experiment, regions of different x-ray exposures (60 kVp spectrum) were created in a single image. To overcome the threshold voltage of the liquid-crystal cell, the XLV was uniformly exposed to radiation prior to formation of the x-ray exposure.

liquid-crystal molecules will experience the electric field caused by the image charge superimposed on the field of the externally applied potential. Alternatively, actinic light emitted onto the photoconductor prior to the formation of an x-ray exposure can also be used to create sufficient charge to overcome the threshold of the liquid-crystal cell.

To be applicable in clinical radiography, the XLV must be sensitive enough to work within an appropriate range of diagnostic x-ray exposures. It must be x-ray quantum noise limited over this range and its resolution must be high. For example, in chest radiography,¹¹ the mean of clinical exposures expected at the detector is 0.3 mR, with an exposure range of 0.03–3 mR. The intensity transfer characteristics of our prototype (Fig. 2) demonstrate that it has the appropriate sensitivity. This experimental prototype consisted of a relatively thin layer of a-Se (150 μm), whereas an optimal device designed for chest radiography would have a thicker a-Se layer to increase quantum efficiency. For example, if the a-Se layer is made 1 mm thick, which is the thickness currently used in flat-panel technology,¹ most of the incident x-rays of the 120 kVp x-ray spectrum used in chest radiography¹¹ will be absorbed. Hence, it is apparent that a radiographic system based on the XLV has the potential to satisfy the previously mentioned criteria.

The fundamental noise sources of our system can be modelled theoretically.¹⁴ It is evident the XLV has the potential to overcome electronic noise in the scanner because the amount of signal can be increased simply by increasing the external illumination level. Small and spatially uniform dark current in the a-Se ensures that the dark current and its noise are negligible compared to the signal charge and its irreducible quantum noise. The high sensitivity of a-Se combined with a negligible dark current ensures sufficient gain, making it possible, in principle, to have an x-ray quantum limited system. Because of its external illumination, sufficient light is available from the XLV and therefore the sensitivity and noise requirements for the optical scanner are modest. In our de-

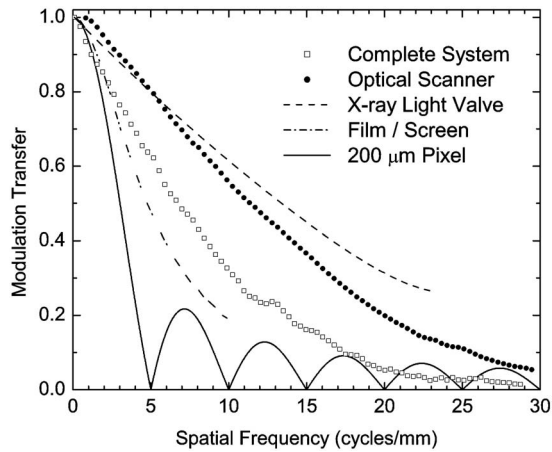


FIG. 3. Modulation transfer functions (MTFs) of the components and the complete imaging chain. The MTFs were measured using the oversampled edge technique (see Ref. 16) in the sensor direction of the scanner. MTF_C of the complete imaging chain (XLV and scanner) is slightly lower than the MTF_S of the optical scanner alone. The inherent resolution of the XLV alone was derived by correcting for the digitization stage (i.e., $MTF_{XLV} = MTF_C / MTF_S$). For comparison, the figure also includes the aperture response of a $200\ \mu\text{m}$ pixel, which defines the resolution requirement for a chest radiography system (Ref. 11), and a very-high resolution film-screen combination (MIN-R 2000/MIN-R2190, Kodak) used in mammographic systems.

vice, a modified paper scanner (CanoScan LiDE 30, Canon) is used. Compared to cameras, scan technology also has the advantage of being very scalable without sacrificing efficiency, image quality, resolution, pixel density, or the low cost of the overall system.

The spatial resolution of the XLV is very high due to the high resolution of a-Se¹⁵ and the very thin liquid-crystal cell ($3.8\ \mu\text{m}$) used. Furthermore, due to the very close proximity of the charge image to the liquid-crystal layer, no significant loss of resolution due to electrostatic spreading occurs. Since the XLV is based on an electrostatic x-ray detector (a-Se) and there is very little resolution lost due to charge spreading during charge collection, high image resolution can be achieved even with photoconductors thick enough to provide high quantum efficiency.¹ This makes it a higher resolution detector than phosphor-based systems whose resolution limit dominantly arises from optical spreading effects.¹ Instead, the inherent spatial resolution limit of a-Se is controlled by the x-ray interactions.¹⁵ In summary, the XLV has the potential to achieve a very high resolution (Fig. 3) as some initial images have demonstrated (Fig. 4).

We have shown that by combining an electrostatic x-ray detector with liquid-crystal technology and an optical scanner, a versatile, high-quality digital radiographic imaging system can be constructed that would be a very attractive alternative for radiology departments. Moreover, since the structure is simple, all elements are based on well-established technologies, and little external circuitry or mechanical support is required beyond conventional computer technology and a high-voltage power supply, the manufacturing costs could be kept significantly lower than competitive digital technologies.

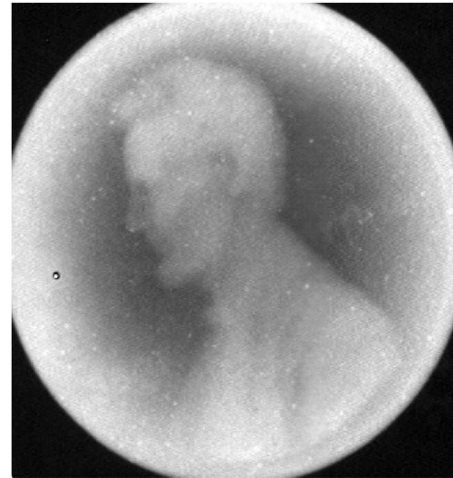


FIG. 4. Example x-ray image of a US penny taken with our prototype acquired at 60 kVp with an exposure to the coin of 27 mR.

This work was supported by the National Institutes of Health Grant No. 5-R01-EB-002-352-02.

^{a)} Author to whom correspondence should be addressed. Electronic mail: john.rowlands@swri.ca

¹ J. A. Rowlands and J. Yorkston, "Flat panel detectors for digital radiography," in *Handbook of Medical Imaging, Vol. 1 Physics and Psychophysics*, edited by J. Beutel, H. Kundel, and R. L. Van Metter (SPIE, Bellingham, 2000), pp. 223–328.

² J. A. Rowlands, "Physics of computed radiography," *Phys. Med. Biol.* **47**, R123–R166 (2002).

³ M. J. Yaffe and J. A. Rowlands, "X-ray detectors for digital radiology," *Phys. Med. Biol.* **42**, 1–39 (1997).

⁴ J. W. May and A. R. Lubinski, "High resolution computed radiography by scanned luminescent toner radiography," *Proc. SPIE* **1896**, 292–312 (1993).

⁵ R. W. Winsor, "Filmless X-ray apparatus and method of using the same," US Patent 5,309,496 (1994).

⁶ J. Grinberg, A. Jacobson, W. Bleha, L. Miller, L. Fraas, D. Boswell, and G. A. Myer, "A new real time non-coherent to coherent light image converter—The hybrid field effect liquid crystal light valve," *Opt. Eng.* **14**, 217–225 (1975).

⁷ D. Armitage, J. I. Thackara, and W. D. Eades, "Photoaddressed liquid crystal spatial light modulators," *Appl. Opt.* **28**, 4763–4771 (1989).

⁸ J. W. Boag, "Xeroradiography," *Phys. Med. Biol.* **18**, 3–37 (1973).

⁹ J. Mort, *The Anatomy of Xerography: Its Invention and Evolution* (McFarland & Co Inc Pub, London, 1989).

¹⁰ W. C. O'Mara, *Liquid Crystal Flat Panel Displays: Manufacturing Science & Technology* (Chapman & Hall, New York, 1993).

¹¹ W. Zhao and J. A. Rowlands, "X-ray imaging using amorphous selenium: Feasibility of a flat panel self-scanned detector for digital radiology," *Med. Phys.* **22**, 1595–1604 (1995).

¹² P. K. Rieppo, B. Bahadur, and J. A. Rowlands, "Amorphous selenium liquid crystal light valve for x-ray imaging," in *Physics of Medical Imaging*, edited by R. L. Van Metter and J. Beutel, *Proc. SPIE* **2432**, 228–236 (1995).

¹³ S. T. Wu and D. K. Yang, *Reflective Liquid Crystal Displays* (Wiley, SID Series in Display Technology, New York, 2005).

¹⁴ P. K. Rieppo and J. A. Rowlands, "X-ray imaging using amorphous selenium: Theoretical feasibility of the liquid crystal light valve for radiology," *Med. Phys.* **24**, 1279–1292 (1997).

¹⁵ W. Que and J. A. Rowlands, "X-ray imaging using amorphous selenium: Inherent spatial resolution," *Med. Phys.* **22**, 365–374 (1995).

¹⁶ E. Samei, M. J. Flynn, and D. A. Reinmann, "A method for measuring the presampled MTF of digital radiographic systems using an edge test device," *Med. Phys.* **25**, 102–113 (1998).